Florida International University

FIU Digital Commons

Department of Psychology | College of Arts, Sciences & Education

9-3-2019

Distinct Neural Circuits Underlie Prospective and Concurrent Memory-Guided Behavior

Amanda G. Hamm

Aaron T. Mattfeld

Follow this and additional works at: https://digitalcommons.fiu.edu/psychology_fac

Part of the Psychology Commons

This work is brought to you for free and open access by the College of Arts, Sciences & Education at FIU Digital Commons. It has been accepted for inclusion in Department of Psychology by an authorized administrator of FIU Digital Commons. For more information, please contact dcc@fiu.edu.

Article

Cell Reports

Distinct Neural Circuits Underlie Prospective and Concurrent Memory-Guided Behavior

Graphical Abstract

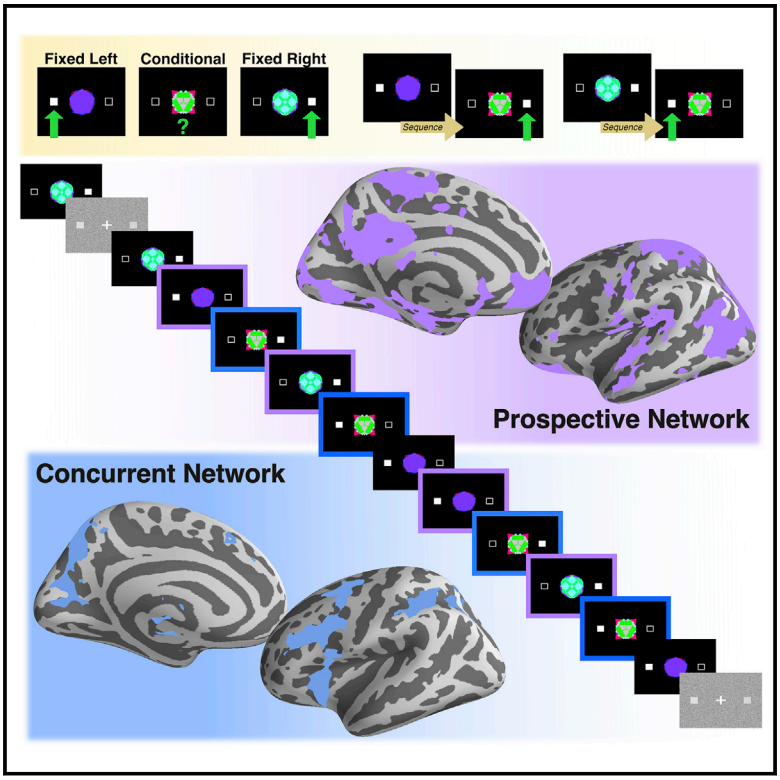

Authors

Amanda G. Hamm, Aaron T. Mattfeld

Correspondence

amattfel@fiu.edu

In Brief

Hamm and Mattfeld use fMRI to demonstrate that greater activations in the hippocampus, medial prefrontal cortex, putamen, and other regions (prospective network) precede successful conditional decisions. In contrast, greater activations in the caudate, dorsolateral prefrontal cortex, and other regions (concurrent network) are associated with the execution of successful conditional behavior.

Highlights

- Use of conditional association task to study the influence of memory on decisions
- Greater prospective network activations precede successful conditional choice
- Execution of conditional choice recruits separate, concurrent network
- Enhanced functional connectivity between hippocampus-mPFC during learning

Hamm & Mattfeld, 2019, Cell Reports *28*, 2541–2553
September 3, 2019 © 2019 The Author(s).
https://doi.org/10.1016/j.celrep.2019.08.002

CellPress

Cell Reports
Article

OPEN ACCESS
CellPress

Distinct Neural Circuits Underlie Prospective and Concurrent Memory-Guided Behavior

Amanda G. Hamm[1] and Aaron T. Mattfeld[1,2,3,*]
[1]Cognitive Neuroscience Program, Department of Psychology, Florida International University, Miami, FL 33199, USA
[2]Center for Children and Families, Florida International University, Miami, FL 33199, USA
[3]Lead Contact
*Correspondence: amattfel@fiu.edu
https://doi.org/10.1016/j.celrep.2019.08.002

SUMMARY

The past is the best predictor of the future. This simple postulate belies the complex neurobiological mechanisms that facilitate an individual's use of memory to guide decisions. Previous research has shown integration of memories bias decision-making. Alternatively, memories can prospectively guide our choices. Here, we elucidate the mechanisms and timing of hippocampal (HPC), medial prefrontal cortex (mPFC), and striatal contributions during prospective memory-guided decision-making. We develop an associative learning task in which the correct choice is conditional on the preceding stimulus. Two distinct networks emerge: (1) a prospective circuit consisting of the HPC, putamen, mPFC, and other cortical regions, which exhibit increased activation preceding successful conditional decisions and (2) a concurrent circuit comprising the caudate, dorsolateral prefrontal cortex (dlPFC), and additional cortical structures that engage during the execution of correct conditional choices. Our findings demonstrate distinct neurobiological circuits through which memory prospectively biases decisions and influences choice execution.

INTRODUCTION

Successful decision-making often requires drawing upon the past. The influence of memory on decision-making has been documented across a diverse array of tasks (Weber et al., 1993; Jadhav et al., 2012; Wimmer and Shohamy, 2012; Zeithamova et al., 2012a; Pfeiffer and Foster, 2013; Gluth et al., 2015; Shohamy and Daw, 2015; Murty et al., 2016; Bornstein et al., 2017; O'Doherty et al., 2017). Much of this research has examined "retrospective-integration" (Shohamy and Daw, 2015) or how experiences containing overlapping content are recalled, combined, and ultimately bias our future choices (Zeithamova and Preston, 2010; Wimmer and Shohamy, 2012; Zeithamova et al., 2012a, 2012b; Gluth et al., 2015; Murty et al., 2016). However, memories can also prospectively guide our choices. The neural mechanisms by which memory prospectively biases our decisions and the timing of those contributions remain central questions.

Memory of our intentions to act in the future, known as prospective memory, has demonstrated the influence of memory on subsequent behavior (Kvavilashvili, 1987; Brandimonte et al., 1996). Most research has focused on strategic monitoring and maintenance of prospective memory cues and have implicated the rostral prefrontal cortex (rPFC; BA10) as an important region for that process (Burgess et al., 2003, 2011; Gilbert et al., 2006; Simons et al., 2006; Haynes et al., 2007; Okuda et al., 2007; Soon et al., 2008; Gilbert, 2011; Benoit et al., 2012; Momennejad and Haynes, 2012, 2013).

Less research has been devoted to the neurobiological mechanisms that support encoding prospective memory (Gilbert, 2011; Momennejad and Haynes, 2012; Cona et al., 2015); however, some computational work suggests prospective memory emerges from interactions between the prefrontal cortex and hippocampus (HPC), with the latter responsible for encoding associations between action plans and the context in which they are to take place (Cohen and O'Reilly, 1996). Research in rodents using spatial tasks strongly supports the role of the HPC through prospective neural signals (Benchenane et al., 2010; Wang and Morris, 2010; Jadhav et al., 2012, 2016; Pfeiffer and Foster, 2013; Euston et al., 2012; Shin and Jadhav, 2016; Yu and Frank, 2015). Based on the ability of the HPC to rapidly acquire relational representations (Eichenbaum and Cohen, 1988; Squire et al., 2004), contribute to future thinking (Addis et al., 2007; Schacter et al., 2017), and support prospective neural coding (Ferbinteanu and Shapiro, 2003), HPC activation would be expected to contribute to prospective memory-guided behavior.

In addition to area BA10, other regions of the medial prefrontal cortex (mPFC) likely contribute to mechanisms of prospective memory, which is due, in part, to structural and functional diversity (de la Vega et al., 2016). Although prospective memory paradigms have shown medial rPFC activation to reflect ongoing tasks, but not delayed intentions (Burgess et al., 2003, 2011; Gilbert et al., 2006; Simons et al., 2006; Benoit et al., 2012), functional decoding analyses have identified additional mPFC regions related to storing of delayed intentions (Haynes et al., 2007; Soon et al., 2008; Gilbert, 2011; Momennejad and Haynes, 2013). Additionally, involvement of the mPFC in maintenance of long-term memories (van Kesteren et al., 2010; Bonnici et al., 2012), integration of memories across episodes (Zeithamova and Preston, 2010), inferential decisions (Zeithamova et al., 2012a), and anatomical connections with the HPC and

This is an open access article under the CC BY-NC-ND license (http://creativecommons.org/licenses/by-nc-nd/4.0/).

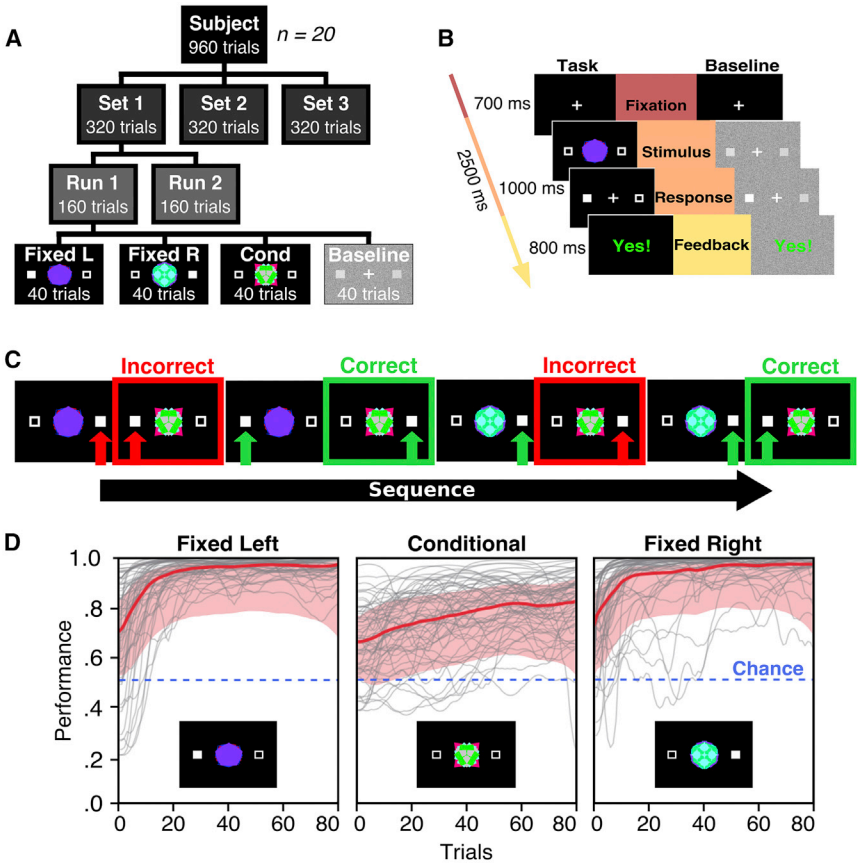

Figure 1. Schematic Diagram of Experiment and Behavioral Results

(A) Total number of trials across experiment categorized by sets, runs, and trial types.

(B) Task and baseline trials were identical in timing (2.5 s) and structure.

(C) Example sequence of events highlighting correct (green arrows and boxes) and incorrect (red arrows and boxes) responses for both fixed and conditional trials.

(D) Performance curves were calculated for each participant across all image sets, producing 60 unique curves (gray lines). Performance was defined as the probability of a correct response on the respective trial. Dark red lines represent mean curves for each stimulus type, whereas the surrounding pink expanse indicates upper and lower bound 95% confidence intervals. Blue dashed lines indicate chance performance of 50%.

pre- and primary motor cortex (Barbas and Blatt, 1995; Cavada et al., 2000; Heidbreder and Groenewegen, 2003; Hoover and Vertes, 2007) all suggest the mPFC is well suited to use memory to guide behavior. Further, research in awake, behaving rodents has identified interactions between the HPC and mPFC related to memory-guided behavior (Benchenane et al., 2010; Shin and Jadhav, 2016; Jadhav et al., 2016), which was prominent during learning (Tang et al., 2017). Thus, we expect both activation in the mPFC and its interactions with the HPC to contribute to prospective memory.

The striatum, also important for decision-making, supports action selection (Balleine et al., 2007). Striatal activity (Tremblay et al., 1998) represents motor preparation, reward expectation, and prediction error (Schultz et al., 2003), all uniquely contributing to instrumental behavior, both response outcome (goal directed) and stimulus response (habitual) (Graybiel, 1995; Yin and Knowlton, 2004; Yin et al., 2005; Liljeholm and O'Doherty, 2012). Notably, prospective memory paradigms rely on stimulus-response associations between prospective cues and specific actions (Einstein et al., 2005; Beck et al., 2014). Taken together, these findings suggest the striatum supports not only prospective biasing of our choices but also execution of those decisions.

The extent to which the HPC, mPFC, and striatum prospectively contribute to memory-guided, conditional behavior in humans, as well as the timing of each, has not been demonstrated. Evidence from statistical learning studies have shown predictive activations in the HPC (Bornstein and Daw, 2012; Schapiro et al., 2012), whereas the mPFC is engaged during events sharing temporal associations (Schapiro et al., 2013). Prospective activations have also been identified in functionally decodable regions of the visual pathway during a multistep reward-learning task (Doll et al., 2015). Striatum activation, specifically in the putamen, has been associated with response preparation and prediction error using similar tasks (Bornstein and Daw, 2012; Doll et al., 2015).

Here, we designed a visuomotor-associative learning paradigm (Petrides, 1997; Law et al., 2005) to examine how the HPC, mPFC, and regions of the striatum (dorsal anterior caudate and putamen) contribute to memory-guided behavior, both before and during conditional decision-making. Participants learned, through trial and error, to associate three stimuli with specific responses. Two images were fixed trials, whose associations were consistent across all presentations. For the third image, or the conditional trial, correct response was dependent on the identity of the preceding trial stimulus. In other words, the correct association for the third image was *conditional* on the previous *fixed* association (Figures 1A–1C). All learning stimuli were presented 80 times across two runs (40 trials per run). A total of three sets of stimuli were learned. Trials lasted 3 s and were as follows: (1) a central fixation cross (700 ms); (2) a kaleidoscopic image and two flanking boxes, during which participants make their selection (1,000 ms); and (3) feedback provided to participants (green, "Yes!" if correct; red, "No!" if incorrect; and white "?" if a response was not received in time) (800 ms). All participants were given instructions on the task and received training outside of the scanner with a set of three unique training images.

With this approach, we investigated the mechanisms of memory-guided behavior. Two distinct neurobiological circuits

emerged: one through which prospective memories are encoded and subsequently bias conditional memory-guided decisions, and a second, which directs execution of the concurrent choice.

RESULTS

Anatomical region of interest (ROI) and exploratory whole-brain analyses tested: (1) differences in prospective activation during fixed trials immediately preceding correct, compared with incorrect, conditional trials to evaluate neurobiological mechanisms of how memory influences conditional decision-making; (2) correlations between first-trial regional activation and second-trial performance for sequential fixed-trial pairs when stimuli either changed or remained the same to further validate whether prospective activations were related to subsequent behavior; (3) prospective functional coupling between anatomically connected regions of interest during periods of learning, compared with periods of non-learning, to corroborate a recent study in rodents that found enhanced functional coupling during learning (Tang et al., 2017); and (4) activation differences between correct conditional and correct fixed association trials to examine differences in brain activations for trials at the time the conditional action was selected.

Behavioral Performance

We found participants were quicker and more accurate on fixed, compared with conditional, trials, and both were performed better than chance. For distributions that violated assumptions of parametric methods (i.e., accuracy and onset of learning), non-parametric Wilcoxon signed-rank and Friedman tests were performed. All results were Bonferroni corrected for multiple comparisons, where appropriate. To determine whether participants performed better than chance, median accuracy was calculated across stimulus sets for each participant. Participants demonstrated significantly better than chance performance for the fixed-right (Fix_R: median = 0.943, interquartile range [IQR]: 0.926 – 0.958; $Fix_{R\ versus\ chance}$: $Z = -3.920$, $p < 0.0001$), fixed-left (Fix_L: median = 0.928, IQR = 0.91 −0.945; $Fix_{L\ versus\ chance}$: $Z = -3.921$, $p < 0.0001$), and conditional images (conditional: median = 0.77, IQR: 0.715 – 0.803; $conditional_{versus\ chance}$: $Z = -3.920$, $p < 0.0001$). When comparing performance across trial types (Fix_R versus Fix_L versus conditional), we observed a significant difference for accuracy ($\chi^2(2, N = 20) = 31.013$, $p < 0.0001$). To determine whether unexpected mnemonic differences exist between fixed-left and fixed-right trials, we compared accuracies. No significant difference between fixed-left and fixed-right trials was observed ($Z = -1.248$, $p = 0.212$). Given the consistent association between stimuli and response for fixed trials, we expected greater accuracy compared with conditional trials. Participants performed significantly better for both fixed-left ($Z = -3.920$, $p < 0.001$) and fixed-right ($Z = -3.920$, $p < 0.001$), compared with conditional trials. A statistically significant difference was observed for response time between the three trial types ($F(2,38) = 29.22$, $p < 0.0001$, partial $\eta^2 = 0.61$). Fixed-left (0.580 ± 0.008 s) and fixed-right (0.588 ± 0.011 s) trials did not significantly differ ($t(19) = -1.086$, $p = 0.291$). However, participants were significantly slower for conditional (0.632 ± 0.009), compared with either fixed-left ($t(19) = -9.429$, $p < 0.001$) or fixed-right ($t(19) = -5.006$, $p < 0.001$), trials. To assess whether conditional performance was related to the depth of processing during fixed trials, we examined whether response time for fixed trials varied as a function of conditional performance. Response times of fixed trials preceding correct conditional trials were not significantly different from those of fixed trials preceding incorrect conditional trials ($t(19) = 0.24$, $p = 0.81$).

Next, we found the onset of learning for conditional trials was delayed compared with fixed-association trials. To evaluate differences in learning between the three stimuli, we calculated learning curves with a logistic regression algorithm designed to assess learning as a dynamic process across trials (Figure 1C; Smith and Brown, 2003; Wirth et al., 2003; Smith et al., 2004). We examined differences in the onset of learning between fixed and conditional trials. The onset of learning was defined as the trial in which the lower-bound 95% confidence interval exceeded chance performance. There was a statistically significant difference in onset of learning between the three trial types ($\chi^2(2) = 22.354$, $p < 0.001$). The onset of learning for fixed-left (median = 3.835, IQR = 2–7) and fixed-right (median = 3.833, IQR = 1–7) trials was not significantly different ($Z = -0.081$, $p = 0.936$). In contrast, the onset of learning was delayed for conditional (median = 11.5, IQR = 6–26), compared with fixed-left ($Z = -3.267$, $p = 0.001$) and fixed-right ($Z = -3.435$, $p = 0.001$) trials.

In summary, no statistically significant differences were observed for accuracy, reaction time, or learning onset between fixed-left and fixed-right trials. Participants, however, were slower to respond, less accurate, and exhibited a delay in learning onset for conditional trials compared to fixed trials. All trial types were performed significantly better than chance.

Prospective Activations of the HPC and Putamen, but Not ACC and Caudate, Differentiate Conditional Trial Performance

Success on conditional trials required participants to remember which of two fixed stimuli had been presented on the preceding trial. We anatomically defined regions of interest bilaterally (HPC, anterior cingulate cortex [ACC], anterior dorsal caudate, and putamen; see STAR Methods) and contrasted level of activation on fixed trials immediately preceding correct and incorrect conditional trials. We predicted the HPC, ACC, and anterior dorsal caudate would exhibit greater prospective activations preceding correct, compared with incorrect, conditional trials given their contributions to relational memory, memory integration, and flexible goal-directed behavior, respectively. In contrast, we expected the putamen to have less of a prospective role.

The HPC and putamen, but not the ACC and anterior dorsal caudate, prospectively differentiated successful conditional memory-guided behavior. Increased HPC activation was observed during fixed trials immediately preceding correct, compared with incorrect, conditional trials (Figure 2A; $t(19) = 3.275$, $p = 0.004$, $d = 0.63$). No significant difference in ACC (Figure 2B; $t(19) = 0.815$, $p = 0.42$) or anterior dorsal caudate (Figure 2C; $t(19) = -1.509$, $p = 0.15$) activation was observed for fixed trials before correct and incorrect conditional trials.

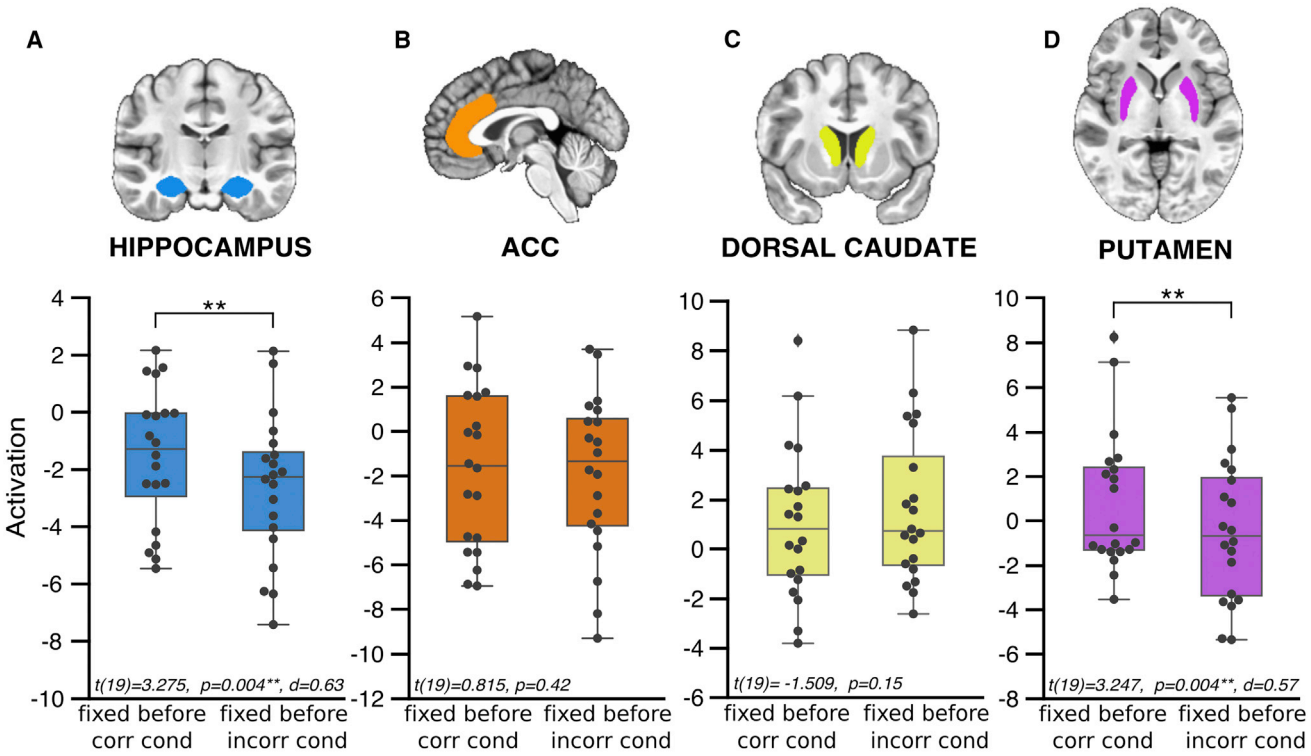

Figure 2. Prospective Activation of the HPC and Putamen, but Not ACC and Caudate, Differentiate Conditional Trial Performance

(A–D) Anatomical regions of interest included: (A) hippocampus, (B) anterior cingulate cortex (ACC), (C) dorsal caudate, and (D) putamen. Boxplots with overlaid swarm plots represent activation for fixed trials preceding the correct (corr cond) and the incorrect (incorr cond) conditional trials. We observed significantly greater activation in the (A) hippocampus and (D) putamen during fixed trials that preceded correct, compared with incorrect, conditional trials. Error bars represent the range of values.

See also Figure S1.

Contrary to our hypothesis, greater putamen activation was observed during fixed trials before correct, relative to incorrect, conditional trials (Figure 2D; t(19) = 3.247, p = 0.004, d = 0.57).

To ensure these findings were not simply a performance artifact from the preceding fixed trial, the same analysis was conducted limiting the scope to correct fixed trials preceding correct and incorrect conditionals. Again, both the HPC (Figure S1A; t(19) = 4.319, p = 0.0004, d = 0.88) and putamen (Figure S1D; t(19) = 2.565, p = 0.02, d = 0.59) exhibited significantly greater activation during fixed trials preceding correct, compared with incorrect, conditional trials. A trend in the ACC (Figure S1B; t(19) = 2.059, p = 0.05) or dorsal anterior caudate (Figure S1C; t(19) = −0.339, p = 0.74) activations were observed.

To provide further mechanistic insight into the nature of prospective signaling in the HPC and putamen, we compared activations for correct-only fixed-left, fixed-right, and conditional trials. If the HPC and putamen contribute to either an encoding or prospective signal, we would expect to observe greater activation in these regions for fixed trials compared with conditional trials. In contrast, if conditional-trial performance is dependent on retrieval-related mechanisms, the opposite pattern (greater activation for conditional, compared with fixed, trials) should emerge. Activations between fixed and conditional trials were significantly different in the HPC (F(2,38) = 10.575, p = 0.001, η^2 = 0.358). Simple effects analysis revealed significantly greater activation for both fixed-left (–1.103 ± 0.45) and fixed-right (–1.266 ± 0.46) compared with conditional (−1.882 ± 0.47) trials (p's < 0.002), whereas no significant difference was found between fixed-left and fixed-right (Figure S2; t(19) = 0.935, p = 0.36). No significant differences were observed for trial type (Figure S2; F(2,38) = 0.211, p = 0.81) in the putamen.

The results of our *a priori* anatomical ROI analysis support the conclusion that prospective HPC and putamen, but not ACC and dorsal anterior caudate, activation are related to successful conditional memory.

Prospective Cortical and Subcortical Activations for Successful Memory-Guided Conditional Behavior

Motivated by the complexities of our conditional memory-guided task and null findings for the ACC—our proxy for the mPFC—an exploratory whole-brain analysis was performed to evaluate potential contributions of additional cortical and subcortical regions to successful conditional memory-guided behavior. We found memory-guided behavior prospectively employs a broad network of cortical and subcortical regions to guide our choices. We searched for voxel-wise differences in activation during fixed trials preceding correct and incorrect conditional trials. We performed a one-sample t test with FSL's software Randomize, with

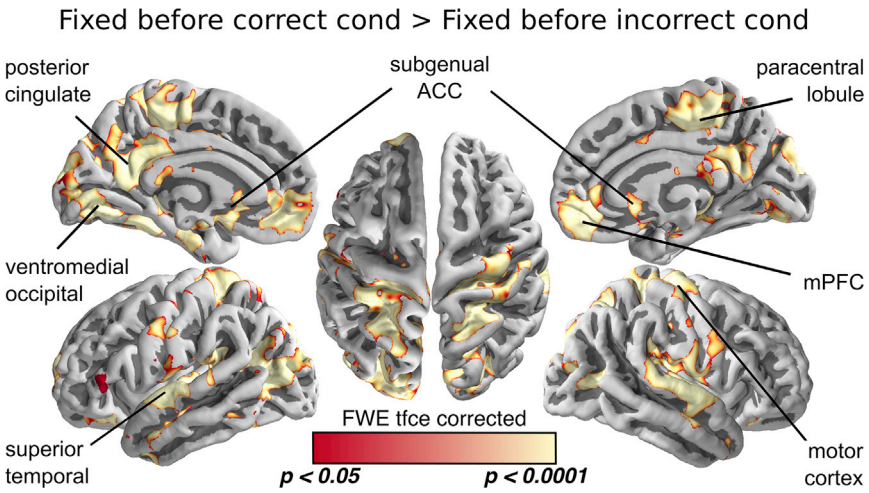

Figure 3. Prospective Cortical Activation for Successful Memory-Guided Conditional Behavior

Cortical regions exhibiting greater activation for fixed trials before correct conditional (cond) trials > fixed trials before incorrect cond trials after whole-brain exploratory analysis (family-wise error [FWE] tfce-corrected $p < 0.05$). Regions of activation included the medial prefrontal cortex (mPFC), posterior cingulate cortex, superior temporal, motor cortex, ventromedial occipital, and the paracentral lobule.

threshold-free cluster enhancement (tfce) correction with a threshold of $p < 0.05$. Consistent with our *a priori* anatomical ROI analysis, clusters along the entire longitudinal axis of HPC and putamen survived correction for multiple comparisons when contrasting greater activation for fixed trials preceding correct conditional trials against fixed trials preceding incorrect conditional trials (Table S1). Additional clusters were observed (Figure 3) for the same contrast in the mPFC (paracingulate cortex extending into medial BA10 and subgenual ACC) and posterior cingulate cortex (PCC), including the retrosplenial cortex, motor cortex, paracentral lobule, superior temporal cortex, ventral visual cortex, and the cerebellum (Figure S3). No regions survived correction for multiple comparisons when contrasting greater activation for fixed trials preceding incorrect conditional trials relative to fixed trials preceding correct conditional trials. Our exploratory results suggest that a widespread cortical and subcortical network prospectively bias conditional memory-guided decisions, including in regions in the mPFC notably anterior to our anatomically defined ROI in the ACC.

Prospective Putamen Activation during Fixed Trials Is Related to Behavioral Performance on Subsequent Trials when Stimulus Is Repeated

In addition to influencing decisions on conditional trials, prospective activations should also bias behavioral performance on subsequent fixed trials, especially when trials repeat. To evaluate the relationship between prospective fMRI activation and subsequent performance for fixed trials, temporally adjacent, fixed trial pairs were selected and sorted according to whether stimuli changed (e.g., fixed left → fixed right) or remained the same (e.g., fixed left → fixed left). Using the same four *a priori* anatomical ROIs, Pearson's correlation coefficients were calculated between regional activation during the first trial and the performance in the second. Beta results were modeled separately for fixed trials, followed by the same or different stimuli. Performance was defined as mean proportion of correct responses for trials that either remained the same (fixed same) or changed (fixed change). We expected fixed trial activation would be related to performance on upcoming fixed trials. To ensure our predictions were not a result of temporal adjacency, we compared activation for conditional trials to the following fixed-trial performance.

We found activation in the putamen for preceding, fixed trials was associated with behavioral performance of the following fixed trials when stimuli remained the same (Figure 4D, right; $r = 0.535$, $p = 0.015$), but not when changed (Figure 4D, left; $r = 0.246$, $p = 0.30$). No significant correlation was observed between HPC activation and performance for fixed-change trials (Figure 4A, left; $r = 0.178$, $p = 0.45$). However, a trend was observed for fixed-same trials (Figure 4A, right; $r = 0.417$, $p = 0.07$). We did not find a significant relationship between ACC activation and performance for fixed-change (Figure 4B, left; $r = -0.205$, $p = 0.39$) or fixed-same (Figure 4B, right; $r = 0.343$, $p = 0.14$) trials. No association between dorsal anterior caudate activation and performance was observed for fixed-change (Figure 4C, left; $r = -0.161$, $p = 0.50$) and fixed-same (Figure 4C, right; $r = 0.063$, $p = 0.79$) trials. Correlations were calculated between activations during conditional trials and the following fixed-trial performance. No significant relationship between conditional activation and subsequent behavioral performance was found (Figures S4A–S4D; all $r < 0.22$, all $p > 0.05$).

Consistent with our hypotheses, prospective fixed-trial activations were associated with subsequent fixed-trial behavioral performance in the putamen, whereas a trend was observed for the HPC. In addition, no similar relationship was identified when comparing conditional activations to upcoming fixed-trial performance.

Prospective HPC-ACC Functional Correlations Are Enhanced during Learning

We examined functional coupling between *a priori* ROIs and known, anatomically connected regions. The HPC directly projects to ACC (Barbas and Blatt, 1995; Cavada et al., 2000); likewise, the dorsal anterior caudate and the putamen receive projections from dorsolateral prefrontal cortex (dlPFC) and the pre- and primary motor cortices, respectively (Künzle, 1975; Selemon and Goldman-Rakic, 1985; Flaherty and Graybiel, 1994; McFarland and Haber, 2000; Haber et al., 2006).

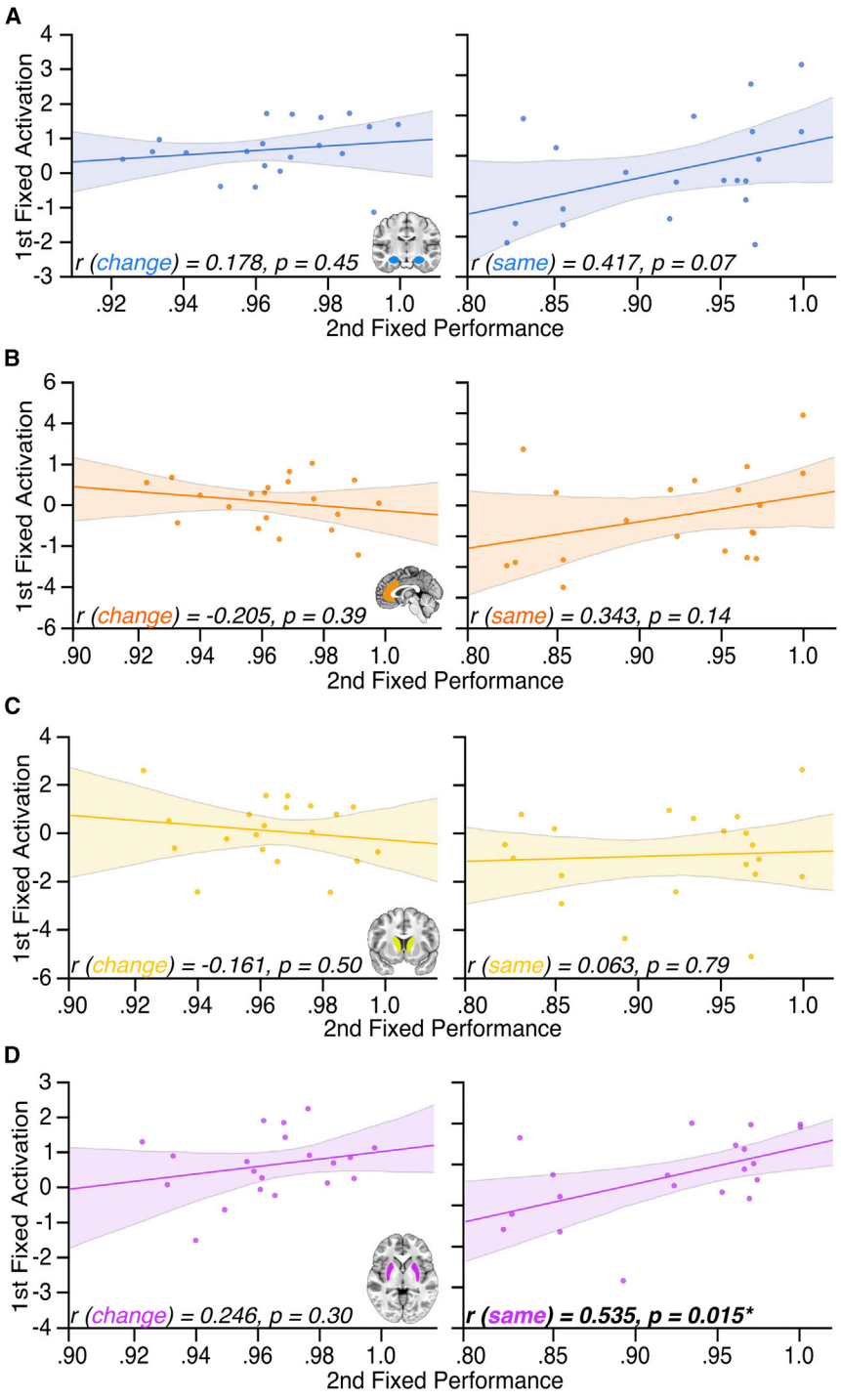

Figure 4. Prospective Putamen Activation during Fixed Trials Is Related to Behavioral Performance on Subsequent Trials When Stimulus Is Repeated

(A) Correlations between preceding fixed-trial activation and subsequent fixed-trial performance for the same (e.g., fixed left → fixed left) and changed (e.g., fixed left → fixed right) trial pairs. A trend was observed between activation in the hippocampus and the fixed-same pairs (right), whereas no significant relationship was observed in the same region for fixed-change pairs (left).

(B and C) No significant correlation between prior fixed activation and subsequent fixed performance was found for the (B) anterior cingulate cortex or (C) dorsal caudate in either change or same pairs.

(D) A statistically significant positive correlation was found for the putamen on fixed-same pairs (right) but not for the fixed-change pairs (left). Clouds along trend line represent the upper and lower 95% confidence interval.

To investigate how functional interactions between these regions support conditional memory-guided behavior, we performed task-based, beta-series correlation analyses (Rissman et al., 2004). A recent study in rodents using an analogous task found increased coherence between the HPC and mPFC during learning, relative to steady-state, behavior (Tang et al., 2017). Thus, we examined functional coupling between three regional pairs during fixed trials preceding conditional trials for periods of learning and non-learning. To operationalize periods of *learning* and *non-learning*, the derivative of the learning curve was calculated across conditional trials. Trials with positive derivative values, representing an increase in performance relative to preceding trials, were considered *periods of learning*. Conversely, *periods of non-learning* were defined as trials in which the derivative was either zero or a negative value, constituting periods of stable or decreased performance. Separate beta series were created with fixed trials preceding learning and non-learning conditional trials; from which, correlations between mean activations of anatomically defined ROIs were calculated. Functional coupling between the HPC and ACC was enhanced during periods of learning (positive derivative: 0.642 ± 0.043) relative to periods of non-learning (negative and/or zero derivative: 0.577 ± 0.049), $t(19) = 2.397$, $p = 0.027$, $d = 0.44$). Conversely, no differences in functional coupling were observed between periods of learning (0.579 ± 0.045) and non-learning (0.579 ± 0.045) for either the dorsal anterior caudate or the dlPFC ($t(19) = 0.230$, $p = 0.821$) or the putamen and pre- and primary motor cortex (positive derivative: 0.716 ± 0.029; negative and/or zero derivative: 0.681 ± 0.028, $t(19) = 1.394$, $p = 0.79$; Figure 5).

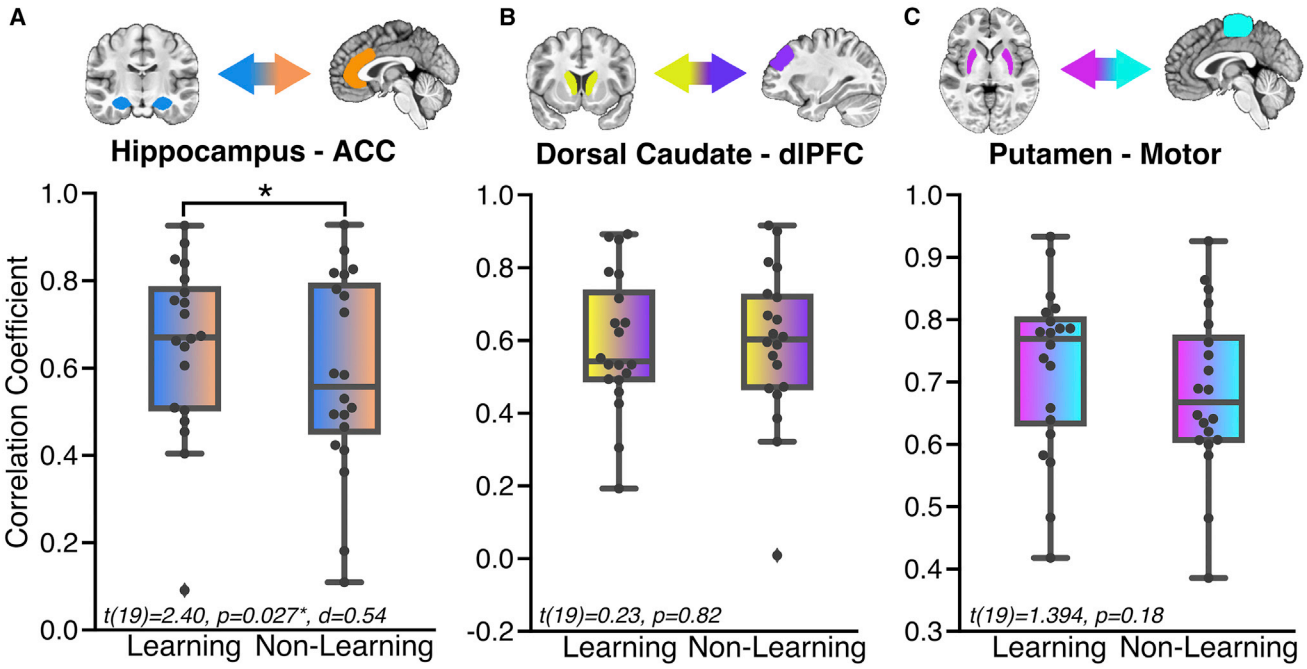

Figure 5. Prospective HPC-ACC Functional Correlations Are Enhanced during Learning

(A–C) Boxplots with overlaid swarm-plots represent distributions of correlations for periods of learning and non-learning between anatomically connected regions of interest. Paired-sample t tests revealed only the hippocampus and anterior cingulate cortex (ACC) exhibited enhanced correlations as a function of learning (A), which was not found for the dorsal caudate and dlPFC (B) or the putamen and motor cortex (C).

Intervening Baseline Trial Representational Dissimilarity in the HPC and mPFC Did Not Correlate with Behavioral Performance on Subsequent Conditional Trials

To further elucidate mechanistic contributions of the HPC and mPFC to prospective memory-guided behavior, we used a multivariate approach to evaluate possible content of HPC and mPFC representations during baseline trials that fell between fixed and conditional trials. The HPC was anatomically delineated, whereas mPFC voxels were defined with a hybrid functional-anatomical mask (see STAR Methods). If activations in these regions reflected maintenance of relevant associations until the conditional cue was presented, conditional performance should be enhanced when pattern dissimilarity between the intervening baseline and the preceding fixed trials was low. In other words, if the pattern of HPC or mPFC activation across voxels during intervening baseline trials was similar to the pattern during typical, fixed, preceding, correct conditional trials, similarities may reflect the maintenance of information; thus, the degree to which such patterns shift would be predictive of impaired performance. We found no relationship between magnitude of pattern similarity for intervening baseline activations with fixed trials preceding correct conditional activations and behavioral performance (HPC: $r = 0.092$, $p = 0.70$; mPFC: $r = 0.188$, $p = 0.43$; Figure S5).

Separate Network Supports Successful Execution of Current Conditional Decision

We found that execution of conditional associations is supported by a wide network of cortical and subcortical regions that are distinct from observed, prospective activations. We performed a second exploratory whole-brain analysis to determine which regions contribute to successful memory-guided behavior during, rather than preceding, correct-conditional associative trials. We compared differences in activation during correct-conditional, compared with correct-fixed, trials (Table S1). We observed greater activation for correct-conditional trials in the bilateral caudate, dlPFC, superior parietal lobule (SPL), anterior insular cortex, and cerebellum (Figure 6). These results reveal a separate network of brain regions important for concurrent-conditional trial performance (e.g., action selection), which contributes to the execution of conditional, memory-guided behavior, beyond those implicated in the preceding fixed trials.

DISCUSSION

We investigated prospective, memory-guided behavior with a conditional-associative learning task. Success on conditional trials was dependent on the stimulus identity from the preceding fixed trial. Using a combination of univariate, multivariate, and connectivity analyses, we identified prospective activations in a network related to successful future decision-making. In addition, a second, separate network associated with successful execution of conditional memory-guided behavior was discovered. These findings demonstrate memory-guided behavior is supported by two distinct neurobiological circuits: one dependent on the HPC, putamen, mPFC, and other cortical regions that prospectively bias subsequent conditional decisions,

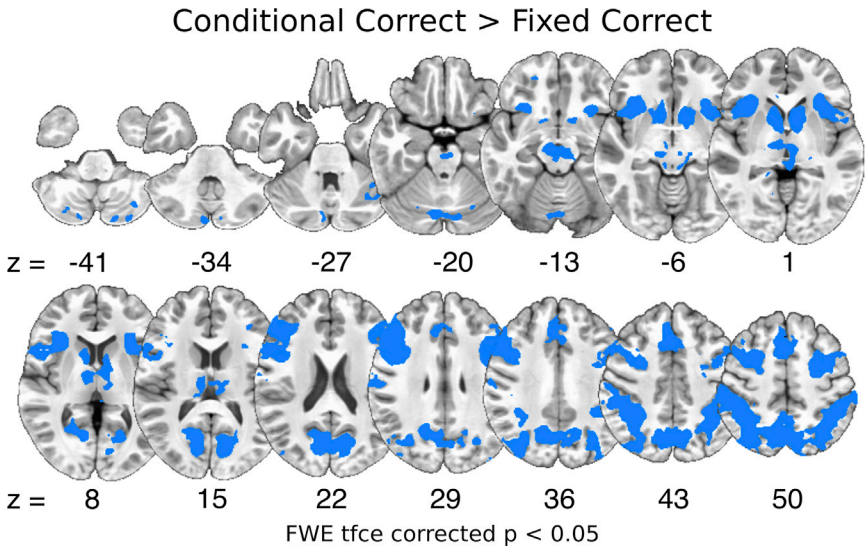

Figure 6. Separate Network Supports Successful Execution of Current Conditional Decision

Cortical and subcortical regions exhibiting greater activation for correct conditional trials compared with correct fixed trials after a whole-brain exploratory analysis (FWE tfce-corrected $p < 0.05$). Regions of activation included the bilateral caudate, dorsolateral prefrontal cortex, pre-supplementary motor area, anterior insula, superior parietal cortex, precuneus, and cerebellum.

whereas the second relies on the striatum, dlPFC, and other cortical regions to use past knowledge for choice execution.

Prospective neural activity constitutes an important mechanism of memory-guided behavior. As expected, HPC activation during fixed trials preceding conditional trials differentiated conditional-trial performance. Notably, in the current task, the HPC is recruited for behavior with very short delays (3 s). Such findings may arise from the highly associative nature of our task because similar HPC outcomes have been identified for relational tasks with short delays (Hannula and Ranganath, 2008) and reflect more temporally compressed contributions when prospective mechanisms are engaged during deliberation (Redish, 2016). An exploratory whole-brain analysis identified a broad network of cortical and subcortical regions with prospective activity, including subregions of the mPFC (paracingulate cortex extending into the BA10 and subgenual ACC), the posterior cingulate cortex extending into the retrosplenial cortex, the superior temporal cortex, the paracentral lobule, and the cerebellum. Surprisingly, the putamen exhibited a similar pattern in activation. The influence of activation in the HPC and putamen was not limited to conditional decisions. We also identified a relationship between fixed-trial activation and subsequent fixed-trial performance in the putamen when stimuli were repeated. In the same analysis, a trend was also observed for the HPC. To gain further insight into mechanistic contributions of the HPC and mPFC, we followed our univariate analyses with a multivariate approach. We used pattern-similarity analysis to determine whether the content of the fixed trials was maintained during the interceding baseline trials. No evidence was found to support a relationship between behavioral performance on conditional trials after intervening baselines and representational similarities in either the HPC or mPFC. The relationships between time, learning, and continuous measurement of performance constitute important limitations. While the motivating goal of our current study was to elucidate neurobiological mechanisms of successful conditional memory guided behavior, these mechanisms may evolve with experience. Future research should examine how learning across time may alter observed neurobiological mechanisms.

Our results extend previous findings in both human and animal literature. Recent studies have identified relationships between prospective fMRI activation and choice. For example, in a study that used a multistep, reward learning task, combined with regionally decodable stimuli, prospective activation of second-stage categories was positively correlated with the degree to which participants used a model-based, relative to a model-free, strategy (Doll et al., 2015). In a sequential learning task in which regularity of adjacent items was manipulated, HPC activation correlated with forward entropy, an estimate of uncertainty of upcoming stimulus conditional on the current one (Bornstein and Daw, 2012). Lastly, activations in the HPC during encoding have been shown to be correlated with the probability that an item was remembered during a later decision phase (Gluth et al., 2015). In the same studies, activations in the putamen were associated with model-free prediction errors (Bornstein and Daw, 2012; Doll et al., 2015) and conditional probability or the degree of response preparation during a sequential learning task (Bornstein et al., 2017). Prospective neural activity constitutes a form of reactivation, which has long been thought to be an important retrieval-related mechanism (Johnson et al., 2009). In a recent action-based learning study, reactivation of medial temporal lobe (MTL) for stimulus triads linked by predictive actions were negatively correlated with stimulus-selective visual-cortex activation (Hindy and Turk-Browne, 2016), suggesting expectations of predictive actions lessen the necessity of sensory processing. The HPC has also been shown to represent prospective rewards during a monetary-incentive encoding task (Zeithamova et al., 2018), and prospective planning signals in the HPC were related to one-shot paired-associate learning in a spatial task (van Kesteren et al., 2018). Spatial navigation studies in rodents have also provided evidence for the role of prospective neural activity for decision-making in the HPC. Awake sharp wave ripple (SWR) events in the HPC reinstate sequential patterns of ''place-cell'' activity of both recent (Foster and Wilson, 2006; Diba and Buzáki, 2007) and remote (Karlsson and Frank, 2009; Gupta et al., 2010) experiences. Further, SWRs are predictive of upcoming choices (Pfeiffer and Foster, 2013), indicative of whether those choices will be subsequently correct or incorrect (Singer et al., 2013). Disruptions of SWRs were

sufficient to impair performance in a continuous alternation task (Jadhav et al., 2012). In the current study, we observed greater activation in the HPC and putamen on trials that preceded correct versus incorrect conditional, memory-guided trials, similar to both results observed in rodents during an analogous spatial-alternation task (Frank et al., 2000; Singer et al., 2013) and statistical learning studies in humans (Bornstein and Daw, 2012). Altogether, and framed within the larger literature, our results suggest the HPC and other regions have an important role in memory representations prospectively guiding decision-making.

The observed activations in our study may reflect a retrieval process important for deliberation at the time of choice (Carr et al., 2011). Evidence suggests prospective activation reflects imagined future options important for upcoming decisions (Addis et al., 2007; Yu and Frank, 2015); however, research in prospective memory provides a compelling alternative. The investigation of prospective memory has been performed within a multiprocess framework that posits prospective remembering is supported by either resource-demanding strategic monitoring or a spontaneous retrieval mechanism (McDaniel and Einstein, 2000; Braver, 2012). Which mechanism prevails is thought to be dependent on the contextual features, such as the task structure (Einstein et al., 2005; Scullin et al., 2010). Many studies provide evidence for a neurobiological mechanism centered on the rPFC, supporting strategic monitoring (Burgess et al., 2003, 2011; Gilbert et al., 2006; Simons et al., 2006; Okuda et al., 2007; Gilbert, 2011; Benoit et al., 2012; Momennejad and Haynes, 2012, 2013). For spontaneous retrieval, the HPC system would be expected to have an important role (Einstein et al., 2005). However, studies of transient responses to prospective memory-target stimuli have not demonstrated HPC activations (Reynolds et al., 2009; Beck et al., 2014). Rather, bilateral HPC activation was observed during encoding of prospective memory intentions (Gilbert, 2011). In the current study, activation in the HPC and other structures during fixed trials proceeding conditionals may reflect encoding of prospective memories. Such an interpretation would be consistent with computational models positing prospective memory results from interactions between the prefrontal cortex and the HPC, the latter being responsible for encoding associations between action plans and future contexts (Cohen and O'Reilly, 1996).

Functional interactions between the HPC and ACC constitute an important mechanism supporting memory-guided conditional behavior modulated by learning. We observed prospective, functional coupling between the HPC and the ACC was enhanced during learning compared with non-learning. Similar differences were not found between either the dorsal anterior caudate and dlPFC, or the putamen and pre- and primary motor cortex. Previous human neuroimaging studies have shown coupling between the HPC and mPFC has a central role in memory-guided decision-making (Zeithamova et al., 2012a; Gluth et al., 2015), memory updating and integration (van Kesteren et al., 2010; Preston and Eichenbaum 2013; Schlichting and Preston, 2016), statistical learning of temporal community structure (Schapiro et al., 2016), and retrieval (Schedlbauer et al., 2014; King et al., 2015). Much of the work in humans has rested on the theory that mPFC guides HPC encoding and retrieval (Preston and Eichenbaum, 2013). The results from our study extend those observations to show such interactions are modifiable through learning. Functional coupling between the HPC and the mPFC in awake, behaving rodents has shown to be an important mechanism in memory-guided behavior (Jones and Wilson, 2005a, 2005b; Benchenane et al., 2010; Remondes and Wilson, 2013; Brincat and Miller, 2015; Yu and Frank, 2015; Jadhav et al., 2016; Guise and Shapiro, 2017; Tang et al., 2017). For example, coupling of spike-timing and theta coherence increases at choice points in mazes, with the degree of coherence modulated by the behavioral performance (Jones and Wilson 2005a, 2005b; Benchenane et al., 2010). We observed enhanced HPC-ACC coupling during learning relative to non-learning periods, similar to a recent rodent study (Tang et al., 2017). In our study, functional interactions between the HPC and ACC may reflect a mechanism by which the ACC modifies HPC activation to facilitate goal-directed behavior. Such a possibility is in line with studies in rodents using a goal-directed paradigm (Guise and Shapiro, 2017).

Activation in the dorsal anterior caudate and related cortical structures (e.g., dlPFC, superior parietal lobule, anterior insula, and precuneus) was associated with successful execution of conditional, memory-guided behavior when compared with correct fixed-association trials. The dorsal anterior striatum represents currently relevant associations of goal-directed behavior. The striatum has long been believed to support instrumental behavior (Graybiel, 1995). Instrumental behavior is dissociable into goal-directed and stimulus-bound or habitual control (Dickinson and Balleine, 1994), with each having been mapped to different neurobiological circuits. Specifically, evidence from animal studies suggests goal-directed behavior is mediated by dorsomedial striatal circuits (Yin et al., 2005), whereas stimulus-bound behavior is supported by dorsolateral circuits (Yin and Knowlton, 2004). A similar functional subdivision has been observed in primates along the anterior-posterior axis (Miyachi et al., 1997, 2002). Neurons in the dorsal anterior caudate modulate firing as goal-directed associations are learned (Tremblay et al., 1998; Blazquez et al., 2002; Miyachi et al., 2002; Hadj-Bouziane and Boussaoud, 2003; Brasted and Wise, 2004), with preceding responses observed in the dlPFC (Pasupathy and Miller, 2005). Similar activations have been observed in humans during instrumental tasks (O'Doherty et al., 2004; Tricomi et al., 2004). In prospective-memory studies, associations between prospective-memory cues and specific actions share many features with instrumental designs. Prior prospective-memory studies have reported transient activation in response to prospective memory-target cues across both cortical and subcortical regions, findings that largely overlap with regions identified in our current study (Simons et al., 2006; Reynolds et al., 2009; McDaniel et al., 2013; Beck et al., 2014). Thus, activation in the dorsal anterior caudate and affiliated cortical structures, for correct conditional greater than correct fixed associations, reflect instrumental goal-directed associations at action selection.

CONCLUSIONS

Taken together, these findings provide evidence for complementary memory processes underlying successful, conditional,

memory-guided behavior. We posit the first of these mechanisms to represent a prospective encoding system that serves to procure and maintain multiple types of representations across experience for future, conditional decisions that are dependent on the HPC and related cortical structures. In addition, we propose a second conditional, memory-guided system that is reliant on the striatum and affiliated cortex, which facilitates concurrent use of past knowledge during choice deliberation. Our findings illustrate successful conditional memory-guided decisions arise from the involvement of multiple learning and memory systems.

STAR★METHODS

Detailed methods are provided in the online version of this paper and include the following:

- KEY RESOURCES TABLE
- LEAD CONTACT AND MATERIALS AVAILBILITY
- EXPERIMENTAL MODEL AND SUBJECT DETAILS
- METHOD DETAILS
  - Behavioral Procedures
  - Prescan Training
  - MRI Methods
- QUANTIFICATION AND STATISTICAL ANALYSIS
  - Anatomical Regions of Interest
  - Task-based fMRI Data Analysis
  - Representational Similarity Analysis
  - Beta-Series Functional Connectivity Analysis
- DATA AND CODE AVAILABILITY

SUPPLEMENTAL INFORMATION

Supplemental Information can be found online at https://doi.org/10.1016/j.celrep.2019.08.002.

ACKNOWLEDGMENTS

Research was conducted with funds provided by FIU. We thank Dr. T. Allen, M. Jayachandran, and J. Hays for useful feedback on the manuscript. We thank M. Farruggia; E. Reyes, RT; and the University of Miami Neuroimaging Suite for assistance in collecting the data.

AUTHOR CONTRIBUTIONS

Conceptualization, A.T.M.; Methodology, A.T.M. and A.G.H.; Investigation, A.T.M. and A.G.H.; Writing – Original Draft, A.G.H. and A.T.M.; Writing – Review & Editing, A.T.M. and A.G.H.; Resources, A.T.M.; Supervision, A.T.M.

DECLARATION OF INTERESTS

The authors declare no competing interests.

Received: February 15, 2019
Revised: June 18, 2019
Accepted: July 30, 2019
Published: September 3, 2019

REFERENCES

Addis, D.R., Wong, A.T., and Schacter, D.L. (2007). Remembering the past and imagining the future: common and distinct neural substrates during event construction and elaboration. Neuropsychologia *45*, 1363–1377.

Avants, B.B., Epstein, C.L., Grossman, M., and Gee, J.C. (2008). Symmetric diffeomorphic image registration with cross-correlation: evaluating automated labeling of elderly and neurodegenerative brain. Med. Image Anal. *12*, 26–41.

Balleine, B.W., Delgado, M.R., and Hikosaka, O. (2007). The role of the dorsal striatum in reward and decision-making. J. Neurosci. *27*, 8161–8165.

Barbas, H., and Blatt, G.J. (1995). Topographically specific hippocampal projections target functionally distinct prefrontal areas in the rhesus monkey. Hippocampus *5*, 511–533.

Beck, S.M., Ruge, H., Walser, M., and Goschke, T. (2014). The functional neuroanatomy of spontaneous retrieval and strategic monitoring of delayed intentions. Neuropsychologia *52*, 37–50.

Benchenane, K., Peyrache, A., Khamassi, M., Tierney, P.L., Gioanni, Y., Battaglia, F.P., and Wiener, S.I. (2010). Coherent theta oscillations and reorganization of spike timing in the hippocampal-prefrontal network upon learning. Neuron *66*, 921–936.

Benoit, R.G., Gilbert, S.J., Frith, C.D., and Burgess, P.W. (2012). Rostral prefrontal cortex and the focus of attention in prospective memory. Cereb. Cortex *22*, 1876–1886.

Blazquez, P.M., Fujii, N., Kojima, J., and Graybiel, A.M. (2002). A network representation of response probability in the striatum. Neuron *33*, 973–982.

Bonnici, H.M., Chadwick, M.J., Lutti, A., Hassabis, D., Weiskopf, N., and Maguire, E.A. (2012). Detecting representations of recent and remote autobiographical memories in vmPFC and hippocampus. J. Neurosci. *32*, 16982–16991.

Bornstein, A.M., and Daw, N.D. (2012). Dissociating hippocampal and striatal contributions to sequential prediction learning. Eur. J. Neurosci. *35*, 1011–1023.

Bornstein, A.M., Khaw, M.W., Shohamy, D., and Daw, N.D. (2017). Reminders of past choices bias decisions for reward in humans. Nat. Commun. *8*, 15958.

M. Brandimonte, G.O. Einstein, and M.A. McDaniel, eds. (1996). Prospective Memory: Theory and Application (Erlbaum).

Brasted, P.J., and Wise, S.P. (2004). Comparison of learning-related neuronal activity in the dorsal premotor cortex and striatum. Eur. J. Neurosci. *19*, 721–740.

Braver, T.S. (2012). The variable nature of cognitive control: a dual mechanisms framework. Trends Cogn. Sci. *16*, 106–113.

Brincat, S.L., and Miller, E.K. (2015). Frequency-specific hippocampal-prefrontal interactions during associative learning. Nat. Neurosci. *18*, 576–581.

Burgess, P.W., Scott, S.K., and Frith, C.D. (2003). The role of the rostral frontal cortex (area 10) in prospective memory: a lateral versus medial dissociation. Neuropsychologia *41*, 906–918.

Burgess, P.W., Gonen-Yaacovi, G., and Volle, E. (2011). Functional neuroimaging studies of prospective memory: what have we learnt so far? Neuropsychologia *49*, 2246–2257.

Carr, M.F., Jadhav, S.P., and Frank, L.M. (2011). Hippocampal replay in the awake state: a potential substrate for memory consolidation and retrieval. Nat. Neurosci. *14*, 147–153.

Cavada, C., Compañy, T., Tejedor, J., Cruz-Rizzolo, R.J., and Reinoso-Suárez, F. (2000). The anatomical connections of the macaque monkey orbitofrontal cortex. A review. Cereb. Cortex *10*, 220–242.

Cohen, J.D., and O'Reilly, R.C. (1996). A preliminary theory of the interactions between prefrontal cortex and hippocampus that contribute to planning and prospective memory. In Prospective Memory: Theory and Applications, M. Brandimonte, G.O. Einstein, and M.A. McDaniel, eds. (Lawrence Erlbaum Associates Publishers), pp. 26–295.

Cona, G., Kliegel, M., and Bisiacchi, P.S. (2015). Differential effects of emotional cues on components of prospective memory: an ERP study. Front. Hum. Neurosci. *9*, 10.

Cox, R.W. (1996). AFNI: software for analysis and visualization of functional magnetic resonance neuroimages. Comput. Biomed. Res. *29*, 162–173.

de la Vega, A., Chang, L.J., Banich, M.T., Wager, T.D., and Yarkoni, T. (2016). Large-scale meta-analysis of human medial frontal cortex reveals tripartite functional organization. J. Neurosci. *36*, 6553–6562.

Diba, K., and Buzsáki, G. (2007). Forward and reverse hippocampal place-cell sequences during ripples. Nat. Neurosci. *10*, 1241–1242.

Dickinson, A., and Balleine, B. (1994). Motivational control of goal-directed action. Anim. Learn. Behav. *22*, 1–18.

Doll, B.B., Duncan, K.D., Simon, D.A., Shohamy, D., and Daw, N.D. (2015). Model-based choices involve prospective neural activity. Nat. Neurosci. *18*, 767–772.

Eichenbaum, H., and Cohen, N.J. (1988). Representation in the hippocampus: what do hippocampal neurons code? Trends Neurosci. *11*, 244–248.

Einstein, G.O., McDaniel, M.A., Thomas, R., Mayfield, S., Shank, H., Morrisette, N., and Breneiser, J. (2005). Multiple processes in prospective memory retrieval: factors determining monitoring versus spontaneous retrieval. J. Exp. Psychol. Gen. *134*, 327–342.

Euston, D.R., Gruber, A.J., and McNaughton, B.L. (2012). The role of medial prefrontal cortex in memory and decision making. Neuron *76*, 1057–1070.

Ferbinteanu, J., and Shapiro, M.L. (2003). Prospective and retrospective memory coding in the hippocampus. Neuron *40*, 1227–1239.

Fischl, B. (2012). FreeSurfer. Neuroimage *62*, 774–781.

Flaherty, A.W., and Graybiel, A.M. (1994). Input-output organization of the sensorimotor striatum in the squirrel monkey. J. Neurosci. *14*, 599–610.

Foster, D.J., and Wilson, M.A. (2006). Reverse replay of behavioural sequences in hippocampal place cells during the awake state. Nature *440*, 680–683.

Frank, L.M., Brown, E.N., and Wilson, M. (2000). Trajectory encoding in the hippocampus and entorhinal cortex. Neuron *27*, 169–178.

Gilbert, S.J. (2011). Decoding the content of delayed intentions. J. Neurosci. *31*, 2888–2894.

Gilbert, S.J., Spengler, S., Simons, J.S., Frith, C.D., and Burgess, P.W. (2006). Differential functions of lateral and medial rostral prefrontal cortex (area 10) revealed by brain-behavior associations. Cereb. Cortex *16*, 1783–1789.

Gluth, S., Sommer, T., Rieskamp, J., and Büchel, C. (2015). Effective connectivity between hippocampus and ventromedial prefrontal cortex controls preferential choice from memory. Neuron *86*, 1078–1090.

Gorgolewski, K., Burns, C.D., Madison, C., Clark, D., Halchenko, Y.O., Waskom, M.L., and Ghosh, S.S. (2016). Nipype: a flexible, lightweight and extensible neuroimaging data processing framework in python. Front. Neuroinform. *5*, 13.

Graybiel, A.M. (1995). Building action repertoires: memory and learning functions of the basal ganglia. Curr. Opin. Neurobiol. *5*, 733–741.

Guise, K.G., and Shapiro, M.L. (2017). Medial prefrontal cortex reduces memory interference by monitoring hippocampal encoding. Neuron *94*, 183–192.e8.

Gupta, A.S., van der Meer, M.A.A., Touretzky, D.S., and Redish, A.D. (2010). Hippocampal replay is not a simple function of experience. Neuron *65*, 695–705.

Haber, S.N., Kim, K.S., Mailly, P., and Calzavara, R. (2006). Reward-related cortical inputs define a large striatal region in primates that interface with associative cortical connections, providing a substrate for incentive-based learning. J. Neurosci. *26*, 8368–8376.

Hadj-Bouziane, F., and Boussaoud, D. (2003). Neuronal activity in the monkey striatum during conditional visuomotor learning. Exp. Brain Res. *153*, 190–196.

Hannula, D.E., and Ranganath, C. (2008). Medial temporal lobe activity predicts successful relational memory binding. J. Neurosci. *28*, 116–124.

Haynes, J.D., Sakai, K., Rees, G., Gilbert, S., Frith, C., and Passingham, R.E. (2007). Reading hidden intentions in the human brain. Curr. Biol. *17*, 323–328.

Heidbreder, C.A., and Groenewegen, H.J. (2003). The medial prefrontal cortex in the rat: evidence for a dorso-ventral distinction based upon functional and anatomical characteristics. Neurosci. Biobehav. Rev. *27*, 555–579.

Hindy, N.C., and Turk-Browne, N.B. (2016). Action-based learning of multistate objects in the medial temporal lobe. Cereb. Cortex *26*, 1853–1865.

Hoover, W.B., and Vertes, R.P. (2007). Anatomical analysis of afferent projections to the medial prefrontal cortex in the rat. Brain Struct. Funct. *212*, 149–179.

Jadhav, S.P., Kemere, C., German, P.W., and Frank, L.M. (2012). Awake hippocampal sharp-wave ripples support spatial memory. Science *336*, 1454–1458.

Jadhav, S.P., Rothschild, G., Roumis, D.K., and Frank, L.M. (2016). Coordinated excitation and inhibition of prefrontal ensembles during awake hippocampal sharp-wave ripple events. Neuron *90*, 113–127.

Jenkinson, M., Beckmann, C.F., Behrens, T.E.J., Woolrich, M.W., and Smith, S.M. (2012). FSL. Neuroimage *62*, 782–790.

Johnson, J.D., McDuff, S.G., Rugg, M.D., and Norman, K.A. (2009). Recollection, familiarity, and cortical reinstatement: a multivoxel pattern analysis. Neuron *63*, 697–708.

Jones, M.W., and Wilson, M.A. (2005a). Theta rhythms coordinate hippocampal-prefrontal interactions in a spatial memory task. PLoS Biol. *3*, e402.

Jones, M.W., and Wilson, M.A. (2005b). Phase precession of medial prefrontal cortical activity relative to the hippocampal theta rhythm. Hippocampus *15*, 867–873.

Karlsson, M.P., and Frank, L.M. (2009). Awake replay of remote experiences in the hippocampus. Nat. Neurosci. *12*, 913–918.

King, D.R., de Chastelaine, M., Elward, R.L., Wang, T.H., and Rugg, M.D. (2015). Recollection-related increases in functional connectivity predict individual differences in memory accuracy. J. Neurosci. *35*, 1763–1772.

Kirwan, C.B., Jones, C.K., Miller, M.I., and Stark, C.E.L. (2007). High-resolution fMRI investigation of the medial temporal lobe. Hum. Brain Mapp. *28*, 959–966.

Künzle, H. (1975). Bilateral projections from precentral motor cortex to the putamen and other parts of the basal ganglia. An autoradiographic study in Macaca fascicularis. Brain Res. *88*, 195–209.

Kvavilashvili, L. (1987). Remebering intentions as a distinct form of memory. Br. J. Psychol. *78*, 507–518.

Law, J.R., Flanery, M.A., Wirth, S., Yanike, M., Smith, A.C., Frank, L.M., Suzuki, W.A., Brown, E.N., and Stark, C.E.L. (2005). Functional magnetic resonance imaging activity during the gradual acquisition and expression of paired-associate memory. J. Neurosci. *25*, 5720–5729.

Liljeholm, M., and O'Doherty, J.P. (2012). Contributions of the striatum to learning, motivation, and performance: an associative account. Trends Cogn. Sci. *16*, 467–475.

Mai, J.K., Assheuer, J., and Paxinos, G. (1997). Atlas of the Human Brain (Academic Press).

MathWorks (2012b). MATLAB and Statistics Toolbox Release (The MathWorks, Inc.).

Mattfeld, A.T., and Stark, C.E.L. (2011). Striatal and medial temporal lobe functional interactions during visuomotor associative learning. Cereb. Cortex *21*, 647–658.

Mattfeld, A.T., and Stark, C.E.L. (2015). Functional contributions and interactions between the human hippocampus and subregions of the striatum during arbitrary associative learning and memory. Hippocampus *25*, 900–911.

McDaniel, M.A., and Einstein, G.O. (2000). Strategic and automatic processes in prospective memory retreival: a multiprocess framework. Appl. Cogn. Psychol. *14*, s127–s144.

McDaniel, M.A., Lamontagne, P., Beck, S.M., Scullin, M.K., and Braver, T.S. (2013). Dissociable neural routes to successful prospective memory. Psychol. Sci. *24*, 1791–1800.

McFarland, N.R., and Haber, S.N. (2000). Convergent inputs from thalamic motor nuclei and frontal cortical areas to the dorsal striatum in the primate. J. Neurosci. *20*, 3798–3813.

Miyachi, S., Hikosaka, O., Miyashita, K., Kárádi, Z., and Rand, M.K. (1997). Differential roles of monkey striatum in learning of sequential hand movement. Exp. Brain Res. *115*, 1–5.

Miyachi, S., Hikosaka, O., and Lu, X. (2002). Differential activation of monkey striatal neurons in the early and late stages of procedural learning. Exp. Brain Res. *146*, 122–126.

Miyashita, Y., Higuchi, S., Sakai, K., and Masui, N. (1991). Generation of fractal patterns for probing the visual memory. Neurosci. Res. *12*, 307–311.

Momennejad, I., and Haynes, J.-D. (2012). Human anterior prefrontal cortex encodes the 'what' and 'when' of future intentions. Neuroimage *61*, 139–148.

Momennejad, I., and Haynes, J.-D. (2013). Encoding of prospective tasks in the human prefrontal cortex under varying task loads. J. Neurosci. *33*, 17342–17349.

Mumford, J.A., Turner, B.O., Ashby, F.G., and Poldrack, R.A. (2012). Deconvolving BOLD activation in event-related designs for multivoxel pattern classification analyses. Neuroimage *59*, 2636–2643.

Murty, V.P., FeldmanHall, O., Hunter, L.E., Phelps, E.A., and Davachi, L. (2016). Episodic memories predict adaptive value-based decision-making. J. Exp. Psychol. Gen. *145*, 548–558.

O'Doherty, J., Dayan, P., Schultz, J., Deichmann, R., Friston, K., and Dolan, R.J. (2004). Dissociable roles of ventral and dorsal striatum in instrumental conditioning. Science *304*, 452–454.

O'Doherty, J.P., Cockburn, J., and Pauli, W.M. (2017). Learning, reward, and decision-making. Annu. Rev. Psychol. *68*, 73–100.

Okuda, J., Fujii, T., Ohtake, H., Tsukiura, T., Yamadori, A., Frith, C.D., and Burgess, P.W. (2007). Differential involvement of regions of rostral prefrontal cortex (Brodmann area 10) in time- and event-based prospective memory. Int. J. Psychophysiol. *64*, 233–246.

Pasupathy, A., and Miller, E.K. (2005). Different time courses of learning-related activity in the prefrontal cortex and striatum. Nature *433*, 873–876.

Peirce, J.W. (2009). Generating stimuli for neuroscience using PsychoPy. Front. Neuroinform. *2*, 10.

Petrides, M. (1997). Visuo-motor conditional associative learning after frontal and temporal lesions in the human brain. Neuropsychologia *35*, 989–997.

Pfeiffer, B.E., and Foster, D.J. (2013). Hippocampal place-cell sequences depict future paths to remembered goals. Nature *497*, 74–79.

Preston, A.R., and Eichenbaum, H. (2013). Interplay of hippocampus and prefrontal cortex in memory. Curr. Biol. *23*, R764–R773.

Redish, A.D. (2016). Vicarious trial and error. Nat. Rev. Neurosci. *17*, 147–159.

Remondes, M., and Wilson, M.A. (2013). Cingulate-hippocampus coherence and trajectory coding in a sequential choice task. Neuron *80*, 1277–1289.

Reynolds, J.R., West, R., and Braver, T. (2009). Distinct neural circuits support transient and sustained processes in prospective memory and working memory. Cereb. Cortex *19*, 1208–1221.

Rissman, J., Gazzaley, A., and D'Esposito, M. (2004). Measuring functional connectivity during distinct stages of a cognitive task. Neuroimage *23*, 752–763.

Roche, A. (2011). A four-dimensional registration algorithm with application to joint correction of motion and slice timing in fMRI. IEEE Trans. Med. Imaging *30*, 1546–1554.

Schacter, D.L., Benoit, R.G., and Szpunar, K.K. (2017). Episodic future thinking: Mechanisms and functions. Curr. Opin. Behav. Sci. *17*, 41–50.

Schapiro, A.C., Kustner, L.V., and Turk-Browne, N.B. (2012). Shaping of object representations in the human medial temporal lobe based on temporal regularities. Curr. Biol. *22*, 1622–1627.

Schapiro, A.C., Rogers, T.T., Cordova, N.I., Turk-Browne, N.B., and Botvinick, M.M. (2013). Neural representations of events arise from temporal community structure. Nat. Neurosci. *16*, 486–492.

Schapiro, A.C., Turk-Browne, N.B., Norman, K.A., and Botvinick, M.M. (2016). Statistical learning of temporal community structure in the hippocampus. Hippocampus *26*, 3–8.

Schedlbauer, A.M., Copara, M.S., Watrous, A.J., and Ekstrom, A.D. (2014). Multiple interacting brain areas underlie successful spatiotemporal memory retrieval in humans. Sci. Rep. *4*, 6431.

Schlichting, M.L., and Preston, A.R. (2016). Hippocampal-medial prefrontal circuit supports memory updating during learning and post-encoding rest. Neurobiol. Learn. Mem. *134* (*Pt A*), 91–106.

Schultz, W., Tremblay, L., and Hollerman, J.R. (2003). Changes in behavior-related neuronal activity in the striatum during learning. Trends Neurosci. *26*, 321–328.

Scullin, M.K., McDaniel, M.A., Shelton, J.T., and Lee, J.H. (2010). Focal/non-focal cue effects in prospective memory: monitoring difficulty or different retrieval processes? J. Exp. Psychol. Learn. Mem. Cogn. *36*, 736–749.

Selemon, L.D., and Goldman-Rakic, P.S. (1985). Longitudinal topography and interdigitation of corticostriatal projections in the rhesus monkey. J. Neurosci. *5*, 776–794.

Shin, J.D., and Jadhav, S.P. (2016). Multiple modes of hippocampal-prefrontal interactions in memory-guided behavior. Curr. Opin. Neurobiol. *40*, 161–169.

Shohamy, D., and Daw, N.D. (2015). Integrating memories to guide decisions. Curr. Opin. Behav. Sci. *5*, 85–90.

Simons, J.S., Schölvinck, M.L., Gilbert, S.J., Frith, C.D., and Burgess, P.W. (2006). Differential components of prospective memory? Evidence from fMRI. Neuropsychologia *44*, 1388–1397.

Singer, A.C., Carr, M.F., Karlsson, M.P., and Frank, L.M. (2013). Hippocampal SWR activity predicts correct decisions during the initial learning of an alternation task. Neuron *77*, 1163–1173.

Smith, S.M., and Brady, J.M. (1997). SUSAN - a new approach to low level image processing. Int. J. Comput. Vis. *23*, 45–78.

Smith, A.C., and Brown, E.N. (2003). Estimating a state-space model from point process observations. Neural Comput. *15*, 965–991.

Smith, A.C., Frank, L.M., Wirth, S., Yanike, M., Hu, D., Kubota, Y., Graybiel, A.M., Suzuki, W.A., and Brown, E.N. (2004). Dynamic analysis of learning in behavioral experiments. J. Neurosci. *24*, 447–461.

Soon, C.S., Brass, M., Heinze, H.J., and Haynes, J.D. (2008). Unconscious determinants of free decisions in the human brain. Nat. Neurosci. *11*, 543–545.

Squire, L.R., Stark, C.E.L., and Clark, R.E. (2004). The medial temporal lobe. Annu. Rev. Neurosci. *27*, 279–306.

Stark, S.M., Frithsen, A., Mattfeld, A.T., and Stark, C.E.L. (2018). Modulation of associative learning in the hippocampal-striatal circuit based on item-set similarity. Cortex *109*, 60–73.

Tang, W., Shin, J.D., Frank, L.M., and Jadhav, S.P. (2017). Hippocampal-prefronal reactivation during learning is stronger in awake compared to asleep states. J. Neurosci. *37*, 11789–11805.

Tremblay, L., Hollerman, J.R., and Schultz, W. (1998). Modifications of reward expectation-related neuronal activity during learning in primate striatum. J. Neurophysiol. *80*, 964–977.

Tricomi, E.M., Delgado, M.R., and Fiez, J.A. (2004). Modulation of caudate activity by action contingency. Neuron *41*, 281–292.

van Kesteren, M.T.R., Fernández, G., Norris, D.G., and Hermans, E.J. (2010). Persistent schema-dependent hippocampal-neocortical connectivity during memory encoding and postencoding rest in humans. Proc. Natl. Acad. Sci. USA *107*, 7550–7555.

van Kesteren, M.T.R., Brown, T.I., and Wagner, A.D. (2018). Learned spatial schemas and prospective hippocampal activity support navigation after one-shot learning. Front. Hum. Neurosci. *12*, 486.

Wang, S.H., and Morris, R.G.M. (2010). Hippocampal-neocortical interactions in memory formation, consolidation, and reconsolidation. Annu. Rev. Psychol. *61*, 49–79, C1–C4.

Weber, E.U., Böckenholt, U., Hilton, D.J., and Wallace, B. (1993). Determinants of diagnostic hypothesis generation: effects of information, base rates, and experience. J. Exp. Psychol. Learn. Mem. Cogn. *19*, 1151–1164.

Wimmer, G.E., and Shohamy, D. (2012). Preference by association: how memory mechanisms in the hippocampus bias decisions. Science *338*, 270–273.

Wirth, S., Yanike, M., Frank, L.M., Smith, A.C., Brown, E.N., and Suzuki, W.A. (2003). Single neurons in the monkey hippocampus and learning of new associations. Science *300*, 1578–1581.

Yin, H.H., and Knowlton, B.J. (2004). Contributions of striatal subregions to place and response learning. Learn. Mem. *11*, 459–463.

Yin, H.H., Ostlund, S.B., Knowlton, B.J., and Balleine, B.W. (2005). The role of the dorsomedial striatum in instrumental conditioning. Eur. J. Neurosci. *22*, 513–523.

Yu, J.Y., and Frank, L.M. (2015). Hippocampal-cortical interaction in decision making. Neurobiol. Learn. Mem. *117*, 34–41.

Zeithamova, D., and Preston, A.R. (2010). Flexible memories: differential roles for medial temporal lobe and prefrontal cortex in cross-episode binding. J. Neurosci. *30*, 14676–14684.

Zeithamova, D., Dominick, A.L., and Preston, A.R. (2012a). Hippocampal and ventral medial prefrontal activation during retrieval-mediated learning supports novel inference. Neuron *75*, 168–179.

Zeithamova, D., Schlichting, M.L., and Preston, A.R. (2012b). The hippocampus and inferential reasoning: building memories to navigate future decisions. Front. Hum. Neurosci. *6*, 70.

Zeithamova, D., Gelman, B.D., Frank, L., and Preston, A.R. (2018). Abstract representation of prospective reward in the hippocampus. J. Neurosci. *38*, 10093–10101.

STAR★METHODS

KEY RESOURCES TABLE

REAGENT or RESOURCE	SOURCE	IDENTIFIER
Software and Algorithms		
PsychoPy2 1.81.02	Peirce, 2009	https://www.psychopy.org
AFNI 16.3.18	Cox, 1996	https://afni.nimh.nih.gov
FSL 5.0.8	FMRIB; Smith et al., 2004; Jenkinson et al., 2012	https://fsl.fmrib.ox.ac.uk/fsl/fslwiki
ANTS 2.1.0	Avants et al., 2008	http://stnava.github.io/ANTs
FreeSurfer 6.0.0	Fischl, 2012	https://surfer.nmr.mgh.harvard.edu
Nipype 1.0.0 dev0	Gorgolewski et al., 2016	https://nipype.readthedocs.io/en/latest/
MATLAB 2013B	MathWorks	https://www.mathworks.com/
SPSS 21	IBM SPSS Statistics	http://www.ibm.com//www.ibm.com/products/
Learning (state-space) algorithm	Smith et al., 2004	http://www.annecsmith.net/behaviorallearning.html
Data analysis scripts	This paper	https://github.com/madlab-fiu/cell_reports_CAT
Deposited Data		
Conditional Association Dataset	OpenNeuro.org	https://openneuro.org/datasets/ds002078/versions/1.0.0

LEAD CONTACT AND MATERIALS AVAILBILITY

Further information and requests for resources and reagents should be directed to and will be fulfilled by the Lead Contact, Aaron T. Mattfeld (amattfel@fiu.edu). This study did not generate new unique reagents.

EXPERIMENTAL MODEL AND SUBJECT DETAILS

Twenty-seven right-handed volunteers performed a conditional visuo-motor associative learning task in a magnetic resonance imaging scanner. All participants provided written informed consent in accordance with local Institutional Review Board requirements. Individuals were recruited from the Florida International University community and financially compensated. Six individuals were excluded from the reported analyses. Three were removed for excessive motion (greater than 20% of time points were flagged as outliers following our outlier detection procedures using 1 mm normalized frame-wise displacement and 3 standard deviations above the mean signal intensity as thresholds). An additional three were removed for poor task performance (lower bound of the 95% confidence interval never exceeded chance performance). Lastly, one participant was removed as a result of experimenter error – first image set was erroneously presented for all six runs. Final sample size was 20 participants (13 females; mean age = 20.82 years, SD = 1.78).

METHOD DETAILS

Behavioral Procedures

The conditional memory-guided associative learning task was modified from a visuomotor associative learning task (Law et al., 2005; Kirwan et al., 2007; Mattfeld and Stark, 2011, 2015; Stark et al., 2018). The experiment was run using PsychoPy2 software (version 1.81.02; RRID: SCR_006571; Peirce, 2009) on a Dell PC computer (Windows 8). Stimuli were back-projected and viewed using an adjustable mirror mounted on the head coil. Participants were presented three unique kaleidoscopic image sets. Each image set was learned across two scanning runs. Participants completed 6 total runs. Each run lasted 6.67 minutes. Stimuli were presented 40 times during each run, for 80 total presentations across 2 runs, resulting in 240 learning stimulus trials per set. Individuals were instructed to learn the association between each image and one of two concurrently presented boxes, which flanked the stimulus, through trial-and-error. Two of three images were associated with either the left or right box exclusively, for which correct response remained consistent across trials. We refer to these trials as *fixed* associative learning trials. The association for the third image, however, was conditional on the identity of the image from the preceding trial and thus could change across trials. We refer to these trials as *conditional* associative learning trials (Figure 1A).

Each learning trial (2500 ms duration) began with the presentation of a centrally located fixation cross for 700 ms, after which a computer-generated kaleidoscopic image (Miyashita et al., 1991) flanked by empty boxes on both the right and left was presented for 1000 ms, during which participants were able to make their selection. Participants responded using their index finger to select the left box and middle finger to select the right box. Responses were recorded using a MR-compatible response box. The chosen box was highlighted to indicate selection. Deterministic feedback (green "Yes!," red "No!," or white ""?) was provided for 800ms after the response.

In addition to learning trials, 40 perceptual baseline (BL) trials were presented to serve as a temporal jitter between trial types, distribute cognitive demand, and provide a reference for the fMRI signal. Sequence and timing of perceptual BL trials was identical to learning trials (Figure 1B). During BL trials participants were presented with a random static pattern image created through binarization of random values for each pixel of screen resolution (1280 × 800). Randomly generated pixel values greater than 0.85 became white, while those below threshold became gray. Placed over this static background, a central white fixation cross was presented, flanked on the left and right by two white outlined boxes. In identical fashion to the larger image, contents of each box were also random static patterns (320 × 200); however, the binarization threshold to produce a white pixel was considerably lower and, for target, vacillated as a function of performance. For the first BL trial, binarization thresholds for target and foil were initially set at 0.55 and 0.65, respectively. Participants were tasked with identifying the "whiter" of the two boxes. If the participant responded correctly to seven out of the previous 10 trials, white threshold for the target box would increase by 10% of that for the last trial, producing fewer white pixels and bringing the image closer to the constant foil threshold of 0.65, thereby increasing task difficulty. Conversely, if response to fewer than five of the preceding 10 BL trials were correct, threshold decreased by 10% of the previous value, leading to a "whiter" target and easier identification.

Prescan Training

All participants received training of 75 total trials (60 learning stimuli and 15 BL trials) using a practice set of three images (two fixed, one conditional) specific to the training session. Training allowed participants to become acquainted with task nature and timing to mitigate loss of trials due to nonresponse at the beginning of the first experimental run. Training was conducted on a MacBook Pro using identical finger-response mapping as scanning session.

MRI Methods

Imaging data were acquired on a General Electric Discovery MR750 3T scanner (Waukesha, WI, USA) with a 32-channel head coil at the University of Miami Neuroimaging Facility (Miami, FL). Functional images were obtained using a T2*-sensitive gradient echo pulse sequence (42 interleaved axial slices, acquisition matrix = 96 × 96 mm, TR = 2000 ms, TE = 25 ms, flip angle = 75°, in-plane acquisition resolution = 2.5 × 2.5 mm, FOV = 240 mm, slice thickness = 3 mm). For each experimental run, 200 whole brain volumes were acquired. Acquisition of imaging data began after the fourth volume to permit stabilization of magnetic resonance signal. A high-resolution, three-dimensional magnetization-prepared rapid gradient echo sequence (MP-RAGE) was collected for purposes of coregistration and normalization (186 axial slices, voxel resolution = 1 mm isotropic, acquisition matrix = 256 × 256 mm, TR = 9.184 ms, TE = 3.68 ms, flip angle = 12°, FOV = 256 mm).

Data were preprocessed and analyzed using the following software packages: Analysis of Functional Neuroimages (AFNI version 16.3.18; RRID: SCR_005927; Cox, 1996), FMRIB Software Library (FSL version 5.0.8; RRID: SCR_002823; Smith et al., 2004; Jenkinson et al., 2012), FreeSurfer (FS version 6.0.0; RRID: SCR_001847; Fischl, 2012), Advanced Normalization Tools (ANTs version 2.1.0; RRID: SCR_004757; Avants et al., 2008), and Neuroimaging in Python (Nipype version 1.0.0.dev0; RRID: SCR_002502; Gorgolewski et al., 2016) pipeline. T1-weighted structural scans underwent cortical surface reconstruction and cortical/subcortical segmentation. Surface reconstruction was visually inspected and errors were manually edited and resubmitted. Functional data were first 'despiked', removing and replacing intensity outliers in the functional time series. We then performed simultaneous slice timing and motion correction (Roche, 2011), aligning all functional volumes to the middle volume of the first run. An affine transformation was calculated to co-register functional data to their structural scan. Motion and intensity outlier time points (> 1 mm frame-wise-displacement; > 3 SD mean intensity) were identified. Functional data were spatially filtered with a 5 mm kernel using *SUSAN* algorithm (FSL; Smith & Brady, 1997), which preserves the underlying structure by only averaging local voxels with similar intensities. The last three volumes of each run were removed to eliminate scanner artifact observed during preprocessing.

Anatomical images were skull-stripped and then registered to MNI-152 template via a rigid body transformation (FSL FLIRT; DOF = 6). This step was used to minimize large differences in position across participants and generate a template close to a commonly used reference. ANTs (Avants et al., 2008) software was used to create a study-specific template to minimize normalization error for any given participant. Each participant's skull-stripped brain was normalized using non-linear symmetric diffeomorphic mapping implemented by ANTS. The resulting warps were applied to contrast parameter estimates following fixed-effects modeling for subsequent group-level tests. To derive MNI coordinates presented in Table S1, the template brain was warped to an MNI template using ANTS and resulting template-to-MNI warps were applied to the outputs from randomize.

QUANTIFICATION AND STATISTICAL ANALYSIS

Anatomical Regions of Interest

Six anatomical regions of interest (ROIs) were bilaterally defined using each participant's structural scan. The hippocampus, putamen, and pre/primary motor cortex (precentral, paracentral, caudal middle frontal, and opercularis labels) were defined by binarizing segmentations from FreeSurfer aparc+aseg.mgz files. The anterior cingulate cortex was also defined using FreeSurfer segmentation (rostral and caudal anterior cingulate labels). We chose to limit our region of interest in the mPFC to the anterior cingulate cortex; admittedly, while the ventral medial prefrontal cortex also receives input from the hippocampal formation, this region was not included due to substantial MRI signal drop-out. The dorsolateral prefrontal cortex was defined using the Lausanne Atlas. The dorsal anterior caudate was manually segmented in accordance with anatomical landmarks outlined in Atlas of the Human Brain (Mai et al., 1997): appearance and secession of the anterior commissure defined the rostral boundary, while the lateral ventricle served as the medial edge and the internal capsule formed the lateral surface. All masks were back-projected to functional space for analysis.

Task-based fMRI Data Analysis

fMRI data were analyzed using FSL based on principles of the general linear model. We used three separate univariate models at first-level to evaluate memory-guided conditional behavior. All models included regressors of no interest which consisted of motion parameters (x, y, z translations; pitch, roll, yaw rotations), first and second derivatives of the motion parameters, normalized motion, first, second, and third order Lagrange polynomials, as well as each outlier time-point that exceeded artifact detection thresholds. In the first model, the regressors of interest consisted of fixed trials that immediately preceded both correct and incorrect conditional trials. All other trial types (i.e., conditional, fixed trials that preceded fixed trials, and fixed trials that preceded baseline trials, baseline trials) were modeled as a single regressor. Contrasts examined differences in activation between fixed trials that preceded correct versus incorrect conditional trials. The second model included regressors of interest for correct and incorrect fixed and conditional trials. The contrast of interest for the second model was differences in activation for correct conditional versus correct fixed trials. The third model included regressors of interest for sequential fixed trial pairs that either shared or changed stimulus from the first to the second trial. The contrast of interest for the third model was differences in activation for the first fixed trial in fixed-same versus fixed-change trial pairs. Event regressors were convolved with FSL's double gamma hemodynamic response function with an onset coinciding with the stimulus presentation and a duration of 3 s. Following first-level analyses, fixed effects analyses across experimental runs were performed for each participant for the respective contrasts of interest. Contrast parameter estimates from fixed effects analysis were normalized to the study specific template and group-level analyses were performed using FSL's *randomize* threshold-free cluster enhancement (tfce) one sample t test ($p < 0.05$).

Representational Similarity Analysis

A representational similarity analysis (RSA) was performed by adding one additional regressor to the first model described in our task-based fMRI analysis. The RSA model contained fixed trials that immediately preceded both correct and incorrect conditional trials, and a new regressor for baseline trials that intervened between fixed and conditional trials as our regressors of interest, as well as regressors of no interest common to our previous models. Similar to the first model, all other trial types (i.e., conditional, fixed trials that preceded fixed trials, and fixed trials that preceded baseline trials, consecutive baseline trials) were modeled as a single regressor. First-level analyses were conducted on unsmoothed data and followed by fixed effects analyses across experimental runs. We calculated correlations between voxel-wise patterns of activation in anatomically defined HPC for fixed trials that preceded correct conditionals versus baseline trials that intervened between fixed and conditional trials. We performed the same analysis using voxels defined by our whole-brain exploratory analysis masked by regions anatomically defined as the medial prefrontal cortex – binarizing Freesurfer labels for rostral and caudal anterior cingulate cortex, superior frontal cortex, and medial orbitofrontal cortex – to isolate regions of the mPFC modulated by task. Using the resulting Pearson's correlation coefficients, we calculated dissimilarity defined as: 1-r. We subsequently correlated our regional dissimilarity measures with behavioral performance during conditional trials that followed the intervening baseline trials.

Beta-Series Functional Connectivity Analysis

A beta-series correlation method (Rissman et al., 2004) was used for our task-based functional connectivity analysis. We employed a least-squares single (LSS) approach (Mumford et al., 2012) given our fast event-related design. Briefly, a separate general linear model was run for each trial of interest. All first level models included a regressor for the single relevant trial, and all remaining task and nuisance regressors with the relevant trial removed from its respective task regressor. Trials of interest were defined by whether they preceded periods of learning or non-learning (conditional trials). We used a logistic regression algorithm (Smith & Brown, 2003; Smith et al., 2004; Wirth et al., 2003), designed to assess learning as a dynamic process observed across trials, to create unique learning curves for each conditional stimulus (MathWorks, 2012b). Utilizing binary responses (correct/incorrect), the learning state process was calculated from the observed outcome of all experimental trials and served to indicate probability of a correct response for any given trial: a metric of learning at each time point of the experimental run. The learning state was defined by obtaining the first derivative of the learning curve for conditional stimuli. If the derivative value was positive, indicating an increase in the probability of being correct relative to the previous trial, it was considered a learning trial. If the value was less than or equal to

zero, representing a decrease or no change in performance, the trial was labeled a non-learning trial. Fixed trials preceding learning and non-learning conditional trials were separately modeled and constructed into a beta-series. *A priori* regions of interest were defined and the average beta-series from each region were correlated. The functional coupling during learning versus non-learning periods was quantified by the degree to which the respective beta-series correlated.

DATA AND CODE AVAILABILITY

The raw magnetic resonance imaging (MRI) datasets generated during this study are available at OpenNEURO.org. The accession number for the data reported in this paper is openneuro: ds002078. The code supporting the current study has been deposited in a public repository on GitHub (https://github.com/madlab-fiu/cell_reports_CAT).